Design and Construction of an Absolute Precision Load/Stress Gauge

Part II. Experimental Methods

Kwang Yul Kim[a]

130 Fieldstone Cir, Ithaca, New York 14850

[a]) kyk1@cornell.edu

[a]) ORCID ID: 0000-0003-1338-5301

ABSTRACT

This paper, Part II of the article series "Design and Construction of an Absolute Precision Load/Stress Gauge," presents implementation of experimental methods for measuring precisely the applied load in absolute units of kg or newton and the applied stress in absolute units of MPa (megapascal). Thus, the Absolute Precision Load/Stress Gauge (APLSG) obviates the need for calibration of the conventional load gauge, which outputs in electrical units, against the dead weight. Both at a stress-free zero load and also at a loaded stressed state, measured are four

[a]) Author's Website: aplgllc.org

quantities: displacement of a load-carrying specimen normal to the vertical loading direction and the three wave speeds of horizontally propagating longitudinal waves, horizontally polarized shear (SH) waves, and vertically polarized shear (SV) waves.

This Part II article provides experimental methods that measures these four quantities with great precision. A long isotropic polycrystalline 7075 aluminum alloy with cylindrical cross-section at zero load is used as a specimen. Initially isotropic shear wave is split into SV and SH mode at a loaded state. The degree of splitting is very small. Therefore, this paper provides methods for precise alignment of the polarization direction of two shear transducers along the vertical and horizontal directions of the uniaxially loaded specimen. Precise alignment is required to obtain the applied load/stress as precisely as possible. In experimental methods use is made of innovative novel techniques or a combination of them and Part II merits as a separate paper, apart from the Part I theoretical paper.

Key Words: Precision Stress Gauge; Absolute Units; Finite Deformation; Thermodynamic Stress; Nonlinear Elastic Deformation; Isothermal Equation of Solids

I. INTRODUCTION

Both theoretical basis and experimental implementation of the Absolute Precision Load Gauge (APLSG) was described in detail in US patent #11-366-003 entitled “Method and Apparatus for an Absolute Precision Load Gauge,”[1], which also describes possible wide

industrial applications. The APLSG requires not only the precise measurement of the wave speed of longitudinal, vertically polarized shear (SV), and horizontally polarized shear (SH) propagating along the horizontal direction in the vertically loaded direction 3 of the load-carrying specimen but also the precise displacement measurement of the specimen along the sound-wave propagating direction 1 or 2. The degree of splitting of the shear wave into the SV and SH modes in the loaded state of an initially isotropic specimen at zero-load state is based on the acoustoelasticity of elastic solids,[2] which indicates very small splitting. Since the polarization direction of the shear transducers used in this experiment is indicated with a few degrees of uncertainty by its vendor, the author feels that the precise alignment of the polarization direction of the shear transducers along the vertical and horizontal directions of the loaded specimen is essential for determination of the load/stress as precisely as possible.

II. GENERAL PROCEDURES

The schematics of the block diagrams of the experimental setup is displayed in Fig. 1. The applied load *P* is exerted on the load-carrying specimen by 300 imperial tons capacity compression machine at the Test Bay of Cornell University. The overall pictorial view of the experimental setup is shown in Fig. 2, where it shows in the center, the compression machine and the load-carrying specimen that is made of a cylindrical block of high-strength7075 aluminum alloy of 122.61 mm cross-sectional diameter and about 360 mm height.
The 7075 aluminum alloy has the yield stress of over 420 MPa and the specimen can be loaded to 480 metric tons without inducing plastic deformation. The 360 mm high circumferential side

wall is shaped with four 19 mm wide flat faces, each 90 degrees apart. Fig. 1 exhibits three L, SV, and SH ultrasonic transducers in contact with the mid-section of the front face of the specimen. The ultrasonic transducers are the products of Panametrics, Inc., which are a broadband transducer with 5 MHz central frequency.

As seen in front of the specimen of Fig. 3, the transducers are held in a jig fixed on the lower aluminum plate. The specimen is placed in the middle of the top surface of the compressor piston and stands through the central holes of upper and lower aluminum plates. Placed on top jig indicated by encircled number 3 is SV polarized shear transducer, located on the middle jig indicated by encircled number 4 is SH polarized shear transducer, and the longitudinal transducer is placed on the bottom jig indicated by encircled number 4. All these transducers are in contact with the 19 mm wide, flat vertical face of the specimen by a weak spring loaded on back of each transducer.

As shown in Fig. 4 is a digital displacement probe A in contact with the flat surface of the rear side of the specimen with a small internal spring force. The probe A indicated by an encircled number 2 is mounted on the upper aluminum plate, which slides with little friction with four linear ball bushings along two circular shafts mounted on the lower aluminum plate, which is separated from the specimen and sits fixed on the flat side bars attached on both sides of inner column walls of the compressor. One mm thick flat microscopic glass slide placed on the front flat surface of the upper aluminum plate is in contact with the front flat surface of the specimen with a small force exerted by a tension spring on the rear side of the specimen, as shown on the bottom of Fig. 4. The tension spring is indicated by encircled number 4.

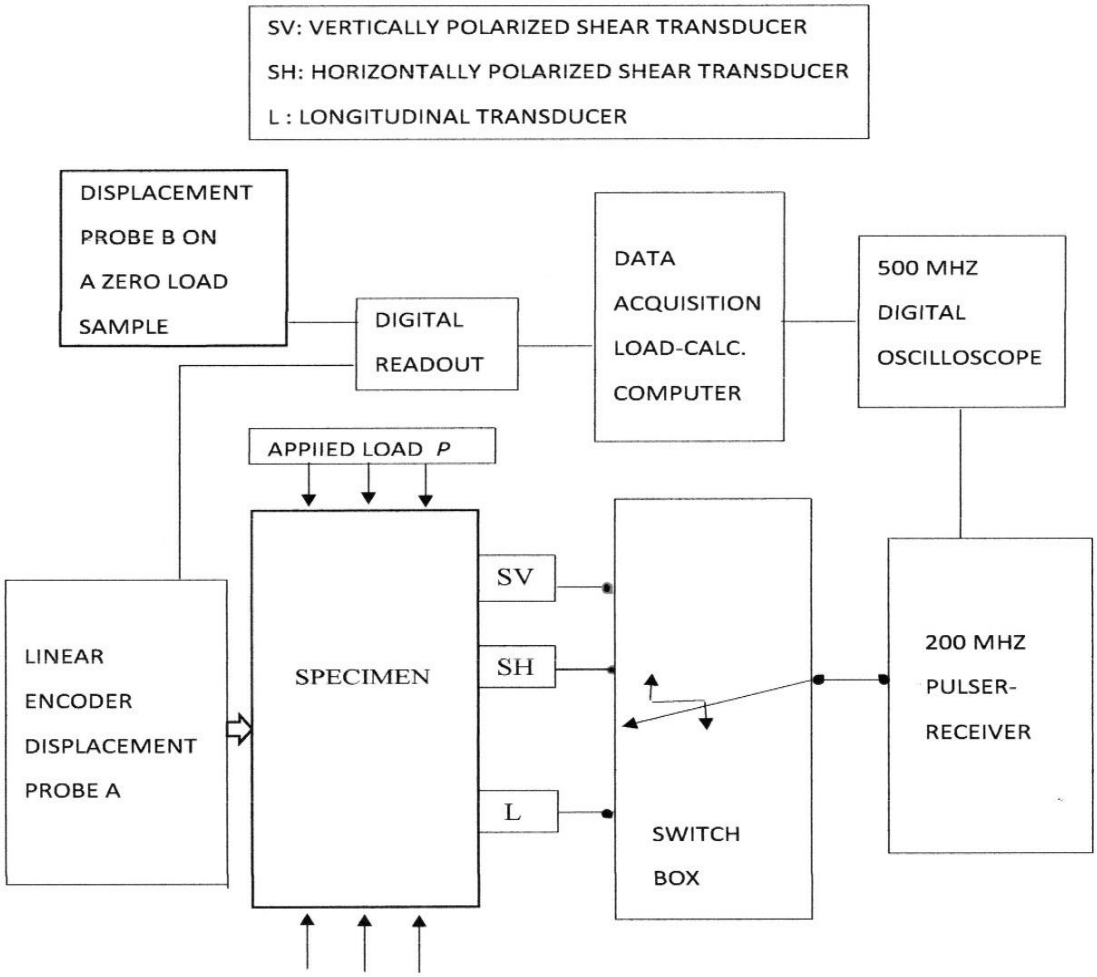

Fig. 1 Schematics of the block diagram of the APLSG experimental setup

Applied load *P* is exerted by the compressor machine

Fig. 2 Overall view of experimental setup

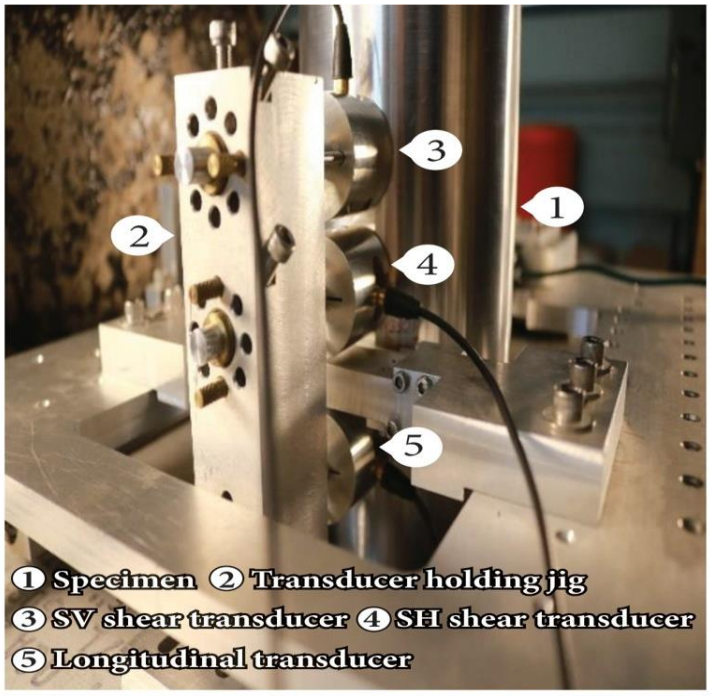

Fig. 3 Front view of a specimen with three jigs of transducers in compression machine

Saint-Venant's principle implies that 360 mm long cylinder length, which is nearly three times the cross-sectional diameter, ensures virtually uniform stress on the midsection of about 70 mm height, where the three transducers and displacement probe are located.

The linear encoder digital displacement probe A is a product of Solartron, Inc., model LE/25/S, which has a displacement span 25 mm and a displacement resolution 50 nm. The dimension of the specimen under load changes as the ambient temperature drifts with time. To compensate for the dimensional variations due to the temperature drift, second probe B identical to the probe A is placed in contact with a zero load sample, which has nearly identical length and is made of the same material

with the specimen under applied load. The probe B is placed next to digital readout meter, model DR600 of Solartron, Inc. They are shown on the left side of the right table in Fig. 2. The outputs of both probes are fed into DR600 in subtraction mode to nearly compensate for the dimensional changes due to temperature drifts. Without the second probe employed, it is desired to minimize the temperature drift less than a few tens of mC^{o}, as 1 C^{o} variation induces 275 nm dimensional change on the specimen. DR600 meter is also capable of displaying the output of the individual probe A or B.

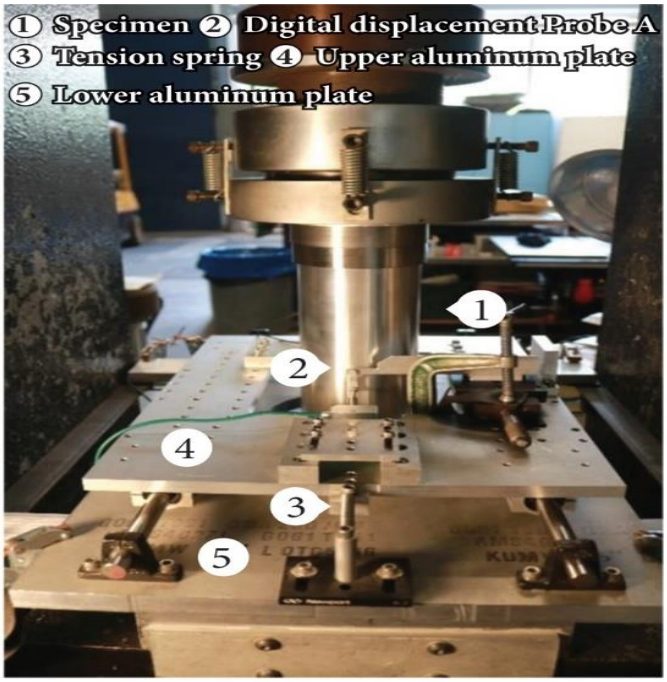

Fig. 4 Rear view of a specimen with a digital displacement probe A and tension spring

200 MHz bandwidth Panametrics pulser-receiver with 5 ns rise time is used to feed excitation pulses to three transducers via a switch box. The sound waves launched from these transducers travel across the specimen, reflect back on the opposite flat face and return to the transducers. They are amplified by the pulser-receiver, and displayed on the 500 MHz Tektronix digital oscilloscope. The round trip travel times of echoed pulses are measured on the oscilloscope with an accuracy of a few parts in 100,000. The oscilloscope signals are brought into digital computer via the GPIB bus of National Instruments, Inc. The oscilloscope and digital computer are placed on the left table in Fig. 2.

The outputs of both probes are fed into DR600 in subtraction mode to nearly compensate for the dimensional change due to the temperature drifts. Without the second probe employed, it is desirable to minimize the temperature drift less than a few tens of mC^o, as 1 C^o variation induces 275 nm dimensional change on the specimen.

Finally, the output of the digital readout is brought into a digital computer, which processes the four measured quantities obtained both at zero load and applied load *P* through MatLab software "CalbFree_LoadCell" written by this author using the formulae shown in Part I: Theory paper. The CalbFree_LoadCell software outputs $C_{11}^T,\ C_{12}^T,\ S_{11}^T,\ S_{12}^T,\ C_{111}^T,$ $C_{112}^T,\ C_{123}^T,\ S_{111}^T,\ \lambda_1,\ \lambda_3, \tau_{33},\ \sigma_{33},$ and finally the applied load *P*.

III. PRECISE ALLIGNMENT OF THE POLARIZATION DIRECTION OF SHEAR TRANSDUCERS

As previously mentioned, the precise alignment of the polarization direction of shear transducers along the vertical and horizontal directions of the loaded specimen is essential for determination of the load/stress as precisely as possible. First, we need to find the polarization direction of the shear transducer. An earlier work for this work was carried out Hsu and Sachse[3], who observed the amplitude of a shear wave to be maximum, when the polarization direction of a shear transducer aligns perpendicular to the stacked glass slides they used as a medium of shear wave propagation. Zuidema and van Soest[4] used <112> direction of a Cu single crystal for shear wave propagation and reported that among the two shear waves observed with the $<\bar{1}10>$ and $<33\bar{4}>$ polarized vibrations, respectively, the shear wave polarized in the latter direction disappears on the oscilloscope screen when the vibration direction of the rotating shear transducer coincides with the $<\bar{1}10>$ direction. The accuracy of these measurements of polarization direction is reportedly about $\pm 5^{o}$. These are the qualitative observations by watching the signals on the oscilloscope screen.

In this paper we choose the <110> direction of a cubic silicon crystal as a propagation direction of the shear wave and describe the quantitative observations of the two shear wave amplitudes with much better accuracy $\pm 0.5^{o}$ for determination of the polarization direction. There is a considerable advantage to using a Si single crystal because of its ubiquitous availability at an affordable price due to widespread semiconductor industries, relatively easy fabrication and polishing of the crystal, and high stability in humid and rusty environments. This was achieved using a Si single crystal, the (001) face of which is oriented in the vertical loading direction**.** The horizontal <110> direction of a silicon single crystal is chosen as the propagation direction to determine the polarization direction of a piezoelectric $Pb(Zr,Ti)O_3$ (PZT) shear transducer used in this experiment. For an arbitrary rotation angle of the transducer against the Si

single crystal, the shear wave is split into the fast transverse (FT) mode polarized in the <001> direction and the slow transverse (ST) mode polarized in the $<1\bar{1}0>$ direction.

In this experiment we used the [110] oriented silicon single crystal disk with 76.2 mm diameter and 38.1 mm thickness in the oriented direction. The [110] orientation of the crystal was determined to an accuracy better than 0.5°. A PZT shear wave transducer of Panametrics, Inc., with 5 MHz bandwidth and 12.7 mm diameter excitation area is mounted on a rotating stage, which has 360 degree division with 60 second resolution for each degree. The transducer is attached on the front (110) surface of the crystal. Throughout the rotating stage of the transducer against the fixed silicon crystal, both the [110] orientation and the [001] direction on the (110) plane of the crystal are maintained to be horizontal and the $[1\bar{1}0]$ direction is kept vertical. Although the 5 MHz PZT shear transducer is used in this experiment, the same method can be applied for determination of the polarization of the crystalline shear transducers aforementioned and any other broadband transducers.

In the [110] propagation direction of a cubic medium, the longitudinal and two shear waves are of pure mode. Their group and phase velocities are equal to each other. For waves launched from a shear transducer with its polarization oriented in an arbitrary direction of the (110) plane, two pure transverse waves are propagating: the fast transverse (FT) with wave-speed of $(C_{44}/\rho)^{1/2}$ = 5.841 mm/μs and the slow transverse (ST) with wave-speed of $[(C_{11}-C_{12})/2\rho]^{1/2}$ = 4.672 mm/μs, where C_{11}, C_{12}, and C_{44} are the elastic constants of silicon and ρ is its density. The vibration directions of the FT and ST waves are the [001] and the $[1\bar{1}0]$, respectively.

Because of these vibration characteristics of the shear waves propagating in the [110] direction of a cubic medium, the amplitudes of the FT and ST waves exhibit maximum when their polarization direction aligns with the [001] and $[1\bar{1}0]$ directions, respectively and they

display minimum when their polarization direction aligns with the $[1\bar{1}0]$ and [001] directions, respectively. The latter criterion, the minimum amplitude, is used to determine the polarization direction, as shown in the following. Because of the two-fold symmetry around the [110] direction of a cubic medium, these minima of each mode are separated by 180°. Since the [001] and $[1\bar{1}0]$ directions are perpendicular to each other, the amplitude minima of the FT and ST waves are separated by 90°. The purpose of this experiment is with what degree of accuracy these minima can be determined as the shear transducer rotates against the fixed silicon crystal.

A 200 MHz pulser-receiver (Panametrics model 5900PR) was used both to feed an excitation signal to the transducer and to amplify the signal that was reflected on the rear (110) surface of the crystal in the pulse-echo mode. The amplified signal was displayed on a digital oscilloscope (Tektronix model TDS 3052) with the bandwidth of 500 MHz, which is capable of exhibiting on the screen a digital readout of the peak-to-peak voltage of the FT and ST waveforms with 8-bit resolution in the measurement mode. The signals on the oscilloscope are obtained after averaging 128 signals to enhance a signal-to-noise ratio.

While the PZT transducer rotates with the polarization direction aligned around the [001] direction on the front (110) plane of the silicon crystal, the amplitudes of the observed FT and ST waves respectively exhibit maximum and minimum. Likewise, when the polarization direction of the shear transducer rotates around the $[1\bar{1}0]$ direction, the amplitudes of the observed FT and ST waves exhibit minimum and maximum, respectively. This behavior is displayed in Fig. 5, which shows that variation of the amplitude of the FT and ST modes with the rotating angle is more sensitive when they go through minimum. This fact can be used to locate the polarization direction of the shear transducer in the digital scope, which displays the peak-to-peak amplitude on the screen. In Figs. 5 and 6, negative angles α is identical with positive angles 360-α.

The minimum amplitude can be used to locate the polarization direction of the transducer with 1^o accuracy with a digital oscilloscope. However, as shown in Fig. 6, the ratio of the amplitude between the FT and ST modes exhibits the resonance-like peaks, when the polarization direction is aligned either along the <001> or along the $<1\bar{1}0>$ direction and can be used to determine the polarization direction of the shear transducer with better than 0.5^o accuracy, which is far better than 5^o accuracy that has been reported to date. This latter method was used to align the polarization direction of shear transducers attached to the specimen along the vertical or horizontal principal stress direction. Details of this method will be published elsewhere.

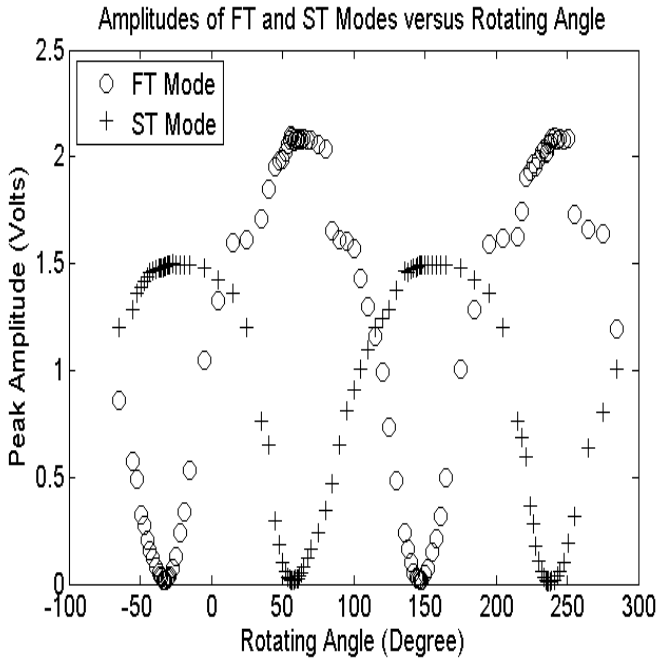

Fig. 5 Amplitude of FT and ST modes vs. rotating angle

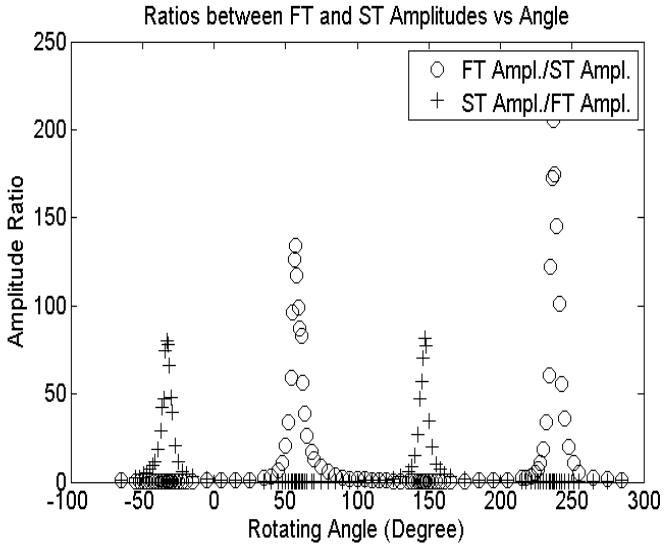

Fig. 6 The ratios between FT and ST amplitudes vs. rotating angle

IV. COMPRESSION TEST RESULTS AND DISCUSSION

As seen in TABLE I, calculated APLSG loads closely match the corresponding compressor loads with a small difference. The compressor load is only approximate, as the compressor machine did not function smoothly and its pressurizing oil medium under the piston leaked slowly during compression, and therefore it was difficult to maintain constant piston pressures. However, the close match between them provides a strong validity to the theory and experimental methods described in this article series. The ultimate test lies in comparing the

output of a strain-gage based load cell recently certified by the National Institute of Science and Technology (NIST) with the APLSG output under the same high capacity loading machine, whether the specimen is in tension or in compression.

The second term $A_a S_{11}^T \tau_{33}{}^2$ in equation *P* (see the bottom of TABLE 1) contributes 0.3% or less to the APLSG load. The third term $A_a\,(S_{111}^T - S_{11}^T)\,\tau_{33}^3/2$ provides a negligible contribution of less than 0.002% to the APLSG load *P* and may be discarded with a desired accuracy 0.01% for the APLSG load. This means that APLSG load is largely determined by $A_a \tau_{33}$ term alone with less than 1% error.

At zero load natural state with ambient temperature 21.7°C, the acoustic path length between two opposite flat faces of the specimen is 121.87 mm and the measured density ρ_a, cross-sectional area A_a and S_{11}^T are

$\rho_a = 2808.3$ kg/m^3 $\quad A_a = 1.1772 \times 10^{-2}$ m^2 $\quad S_{11}^T = 1.4048 \times 10^{-11}$ (Pa)$^{-1}$

TABLE 1 The values of S_{111}^T, τ_{33} , σ_{33} , and APLSG load obtained by CalbFree_LoadCell software program at four different compressor loads.

Compressor Load (Imperial Ton)	S_{111}^T ($10^{-21}(Pa)^{-2}$)	τ_{33} (MPa)	σ_{33} (MPa)	APLSG Load P^* (Imperial Ton)
~ 100	3.2623	79.833	79.684	105.543
~ 150	3.2760	117.60	117.28	155.393
~ 200	3.2786	155.72	155.16	205.659
~ 250	3.3613	193.22	192.36	255.047

$$^*P = A_a \tau_{33}\left[1 + S_{11}^T \tau_{33} + (1/2)\left(S_{111}^T - S_{11}^{T\,2}\right)\tau_{33}{}^2 + \cdots\right]$$

Ordinary engineering polycrystalline materials exhibits a slight anisotropy, which is difficult to characterize. During the manufacturing processes they may be heat-treated and also rolled. Rolling process induces texture in the rolled material and some of textured materials may be characterized as possessing nearly isotropic but slightly transversely isotropic symmetry about the rolled direction. One should choose a loading direction 3 that coincides with the axis of transverse isotropy of the textured specimen. The transversely isotropic material has five second order elastic constants, which can easily be determined at zero load natural state to calculate S_{33}^T in Eq. 18, S_{12}^T and S_{13}^T. The transversely isotropic material possesses a total of 9 third order elastic (TOE) constants, each of which are usually measured with a significant error.

Determination of S_{333}^Tvia Eq. 4b is unyielding and involves a large error. However, noting that $(S_{333}^T - S_{33}^T)\tau_{33}^2/2$ in Eq. 18 makes a negligible contribution to applied load *P*, nine TOE constants of a weakly transversely isotropic but nearly isotropic specimen may be reduced to three isotropic TOE constants. Referring to Ref. 6, one replaces C_{113}^T byC_{112}^T , $C_{144}^T = C_{155}^T = C_{344}^T$ by $(C_{112}^T - C_{123}^T)/4$, C_{133}^T by C_{112}^T and C_{333}^T by C_{111}^T. For a transversely isotropic material one replaces in Eqs. 8b-16 all S_{12}^T by S_{13}^T and all S_{11}^T by S_{33}^T and derives modified equations equivalent to Eqs. 12a, 12b, and 12c involving three TOE constants C_{111}^T ,C_{112}^T , and C_{123}^T . Then, τ_{33}, $C_{111,}^T$ C_{112}^T , and C_{123}^T for a weakly transversely isotropic material can be obtained in a similar manner used in the previous section. Using Eq. 4b yields S_{333}^T in Eq. 18. With the knowledge of τ_{33}, S_{33}^T, and S_{333}^T one can finally obtain the applied load for a slightly transversely isotropic specimen. A similar approach can be extended to a slightly orthotropic specimen. The details of the texture effects on the APLSG load lie outside the scope of this work and will be treated elsewhere.

A more suitable specimen material may be chosen with amorphous isotropic fused

quartz, because it has higher acoustoelastic constants due to its low density (2202 kg/m^3) less than that of 7075 aluminum alloy, and because difference between its isothermal and adiabatic values are very small due to its low thermal expansion coefficient and may be safely ignored. Therefore, fused quartz with about 100 mm cross-sectional diameter may be an ideal candidate. The drawback is that it is expensive to manufacture and fabricate such a large quartz. Another ideal specimen candidate may be a (001) oriented single crystal of silicon with about 100 mm diameter cross-sectional area. The theory in Section II can be extended without difficulty to a cubic single crystalline specimen with necessary additional measurements of the sound waves propagating in the [100] and [110] directions.

Three piezoelectric ultrasonic transducers used in this experiment are a contact type, which requires a slight lateral stress on the specimen to provide a solid coupling. This coupling pressure problem can be overcome by adopting non-contact type ultrasonic transducers, such as a dual mode EMAT (electromagnetic acoustic transducer) with a single magnet and a pancake coil described by Hirao and Ogi[5]. This type of EMAT is capable of measuring the sound speeds of L, SV, and SH waves with a single EMAT and may be ideally suited for construction of the APLSG. The better accuracy and resolution in lateral displacement can be achieved by adopting a laser interferometric technique.

The APLSG can find wide industrial applications[1]. First, the APLSG can replace or calibrate the load cells, which output in electrical units and which are currently in wide use. Companies dealing with heavy metals, such as US steel Inc. and Alcoa aluminum Inc. etc., frequently ship heavy metals weighing 100 tons or more to their customers and shipping them with about 1 % error will cost these companies lots of money. Using the APLSG can minimize error in weight measurement and save lots of money. Similar cost savings happen when they

load and unload the freights at the shipping dock from the transportation ship at the harbor. Numerous truck inspection stations throughout the US high ways can use the APLSG to minimize the errors in weight measurement of freight trucks weighing more than tens of tons.

V. CONCLUSIONS

1. Experimental results indicate that the linear term of thermodynamic stress, $A_a\tau_{33}$, (see Eq. 18 in Part I of this article series) contributes more than 99% to the applied load P and applied Cauchy stress σ_{33} in the APLSG. The second term $A_a E(\mathbf{a})^{-1}{\tau_{33}}^2$ contributes less than 1% in the APLSG, where third term makes a negligible contribution.

2. The formula in Eq. 18 in Part I of this article series shows that calculation of the applied load can be applicable to a nearly isotropic specimen with slightly orthotropic or weakly transversely isotropic symmetry. The loading direction should be chosen so as to coincide with one of symmetry axes of the specimen. A textured specimen may possess one of these classes of symmetry[6]. Eq. 6c in the Part I paper applies to an isotropic specimen.

3. The texture effects and inhomogeneity of ordinary engineering polycrystalline materials can be circumvented by choosing an amorphous specimen material such as fused quartz or a single crystal such as [001] oriented silicon.

4. Digital displacement probe A indicated by encircled number 2 in Fig. 4 has 50 nm displacement resolution. However, with the rapid progress in nanofabrication technique, we may

see soon a displacement probe with better than 10 nm resolution with evermore precision in the APLSG gauge.

ACKNOWLEDGMENTS

This work was initiated and financed by the article's sole author, Kwang Yul Kim. The design of mechanical parts, set up of mechanical assembly, electronic instrumentation, measurements of displacement and ultrasonic wavespeeds, were all carried out by the author.

The author expresses sincere gratitude to Mr. Steve Keast for his technical assistance for the fabrication of the APLSG apparatus and to Mr. James Strait for testing the APLSG at the Test Bay of Cornell University.

REFERENCES

[1]Kwang Yul Kim, Inventor, "Method and Apparatus for an Absolute Precision Load Gauge," US Patent #11,366,003. Granted on June 21, 2022.

[2]K.Y. Kim and W. Sachse, in *Handbook of Elastic Properties of Solids, Liquids, and Gases,* edited by Levy, Bass, Stern, Vol. 1, edited by A.G. Every and W. Sachse, Chap. 19, pp. 441-468 (Academic, San Diego, 2001).

[3]N.N. Hsu and W. Sachse, "Generation and detection of plane-polarized ultrasound with a rotatable transducer," Rev. of Sci. Instrum. **46** (1975), pp., 923-926. https://doi.org/10.1063/1.1134356

[4]J. Zuidema and Th.M. van Soest, "An acoustic determination of the direction of the vibration of ordinary acoustic shear wave transducers," J. Nondestr. Eval. **3** (1982), pp.77-84. https://doi.org/10.1007/BF00568963

[5]Masahiko Hirao and Hirotsugu Ogi, *EMATS for Science and Industry*: *Noncontacting Ultrasonic Measurements* (Kluwer Academic, Boston, 2003).

[6]R.F.S. Hearmon, in *Numerical Data and Functional Relationships in Science and Technology*, edited by K.-H. Hellwege and A.M. Hellwege, Landolt-Börnstein, New Series, Group III, Vol. 11 (Springer-Verlag, New York, 1979).